Cytoprotective Effects of the Lipoidic-Liquiform Pro-Vitamin C Tetra-Isopalmitoyl-Ascorbate (VC-IP) Against Ultraviolet-A Ray-Induced Injuries in Human Skin Cells Together With Collagen Retention, MMP Inhibition and p53 Gene Repression

Li Xiao,[1] Kentaro Kaneyasu,[1] Yasukazu Saitoh,[1] Yoichi Terashima,[2] Yasunori Kowata,[3] and Nobuhiko Miwa[1]*

[1]*Laboratory of Cell Death-Control BioTechnology, Faculty of Life and Environmental Sciences, Prefectural Hiroshima University; Nanatsuka 562, Shobara, Hiroshima 727-0023, Japan*
[2]*Tokyo Metropolitan Police Hospital; Nakano 4-21-1, Nakano-ku, Tokyo 164-8541, Japan*
[3]*Nikko Chemicals Cosmos Technical Center; Hasune 3-24-3, Itabashi-ku, Tokyo 174-0046, Japan*

ABSTRACT

Irradiation with ultraviolet-A (UVA) ray at doses of 20–100 J/cm^2 diminished the cell viability of human keratinocytes HaCaT and human melanoma cells HMV-II, both of which were protected by pre-irradiational administration with the ascorbic acid (Asc) derivative, VC-IP (2,3,5,6-O-tetra-2′-hexyldecanoyl-L-ascorbic acid; vitamin C-isopalmityl tetraester), which is the first lipoidic-liquiform pro-vitamin C by itself that is materialized by esterization of all four intramolecular hydroxyl groups of an Asc molecule with branched chain fatty groups, resulting in molecular fluidity higher than that of the corresponding straight chains. Irradiation with UVA to HaCaT keratinocytes was shown to cause the formation of 8-hydroxydeoxyguanosine (8-OHdG), translocation of phosphatidylserine in the inner layer into the outer layer of cell membrane, and lowering of a mitochondrial membrane potential, all of which were repressed by pre-irradiational administration with VC-IP. Expression of p53 gene, another hallmark of UV-induced DNA damages, was promoted by UVA irradiation to the keratinocytes but also repressed by VC-IP. Administration with VC-IP of 10–50 μM to human fibroblasts NHDF achieved the enhancement of collagen synthesis, repression of matrix metalloprotease-2/9 activity, and increasing of intracellular Asc contents more markedly than that with Asc itself of the same concentrations. Thus UVA-induced diverse harmful effects could be prevented by VC-IP, which was suggested to ensue intrinsically from the persistent enrichment of intracellular Asc, through esterolytic conversion of VC-IP to a free-form Asc molecule, resulting in relief to UVA-caused oxidative stress. J. Cell. Biochem. 106: 589–598, 2009.   © 2009 Wiley-Liss, Inc.

KEY WORDS: 2,3,5,6-O-TETRA-2′-HEXYLDECANOYL-L-ASCORBIC ACID; UVA; CYTOPROTECTION; 8-OHDG; APOPTOSIS; COLLAGEN SYNTHESIZE; MMPs

Premature senescence of the skin including photoaging is a well-documented consequence of frequent exposures to intense or repeated UV irradiation. The exposure of skin to UV ray will induce the extensive generation of reactive oxygen species (ROS) within the intracellular space, typically for UVA or occasionally for UVB. The oxidative stress is involved in the damage of cellular constituents, such as DNA, cell membrane lipids, proteins or fatty acids and saccharides. This theory is supported by the presence of both 8-OHdG which is the marker of oxidative modification of DNA-base, and oxidatively modified proteins such as 4-hydroxy-2-nonenal-modified amino acids, 3-L-nitro-tyrosine and N (-epsilon) (carboxymethyl) lysine in UV-exposed skin specimens [Fisher et al., 2002; Yu et al., 2006; Negishi et al., 2007]. ROS-induced molecular injuries will result in a number of harmful effects on cellular functions and homeostasis. One of these processes can lead to distinct changes in skin connective tissue by degradation of extracellular matrix (ECM) proteins such as collagen. The production of matrix metalloproteinases

(MMP) by UV-irradiated skin fibroblasts and the resultant ECM degradation by these enzymes were known to be included in the main causes of photoaging [Wlaschek et al., 1995; Ichihashi et al., 2003; Sudel et al., 2003; Kim et al., 2004; Honda et al., 2008]. Otherwise, UVA-induced ROS generation also appeared to enhance a common final pathway that involved signaling through the tumor suppressor gene p53 which is more specifically to DNA damage to cause apoptosis [Liardet et al., 2001; Molho-Pessach and Lotem, 2007].

One approach to protect human skin against the harmful effects of UV irradiation is to use antioxidants. The representative antioxidant is ascorbic acid (Asc) which has been used in skin care preparations as a scavenger of ROS to prevent UV-irradiational injures. Asc and its derivatives have been shown to protect against sunburn, delay the onset of skin tumors, and reduce UV-induced skin wrinkling [Thomas et al., 2001; Besaratinia et al., 2007]. It is a pity that, despite having these desired properties, Asc has not been used for cosmetic formations successfully owing to its weak stability and poor solubility in oily materials. Several liposoluble derivatives of ascorbic acid have shown a significant stability and ROS-scavenging activity. However, as conventional cosmetic materials, those liposoluble Asc derivatives were not liquiform in a pure form, but powder by itself that hampers their ability when mixed with other cosmetic ingredients [Kurata et al., 1993; Tai et al., 2003].

We have developed the first derivative of Asc that is liquiform by itself as 2,3,5,6-O-tetra-2′-hexyldecanoyl-L-ascorbic acid designated as vitamin C-tetra-isopalmitate (VC-IP), which is esterized at all four intramolecular hydroxyl groups with branched chain fatty groups that are more fluid than the corresponding straight fatty chain (Scheme 1). VC-IP has already been widely utilized as a medical additive in the cosmetic field for years, but remains to be analyzed from a viewpoint of molecular and cellular pharmacology.

In the present study, 2,3,5,6-O-tetra-2′-hexyldecanoyl-L-ascorbic acid was synthesized and evaluated for the thermal stability, solubility and cytotoxicity. At the same time, the cytoprotection of VC-IP on UVA-induced injures in the human skin cells, the ability to promote collagen synthesis and cell-membrane permeability were also investigated.

MATERIALS AND METHODS

PREPARATION OF VC-IP

2,3,5,6-O-Tetra-2′-hexyldecanoyl L-ascorbic acid (VC-IP) was prepared as follows: 2-Hexyldecanoyl chloride (128.8 g, 469 mM) was added to a 0–5°C solution of L-ascorbic acid (18.3 g, 104 mM) and pyridine (74 g, 935 mM) in DMF (120 ml) under N_2 and left to react for 1 h. The mixture was extracted with hexane (180 ml), the organic layer was washed with 5% HCl (50 ml), H_2O (3 × 150 ml), dried ($MgSO_4$) and evaporated. The residual product was purified by silica gel column chromatography using n-hexane/benzene (4:1) as the eluent. The structure of the product was identified by ^{1}H-NMR (CDCl$_3$), ^{13}C-NMR and IR. VC-IP was obtained as a clear and colorless liquid. The structure was identified by ^{1}H-NMR (CDCl$_3$), ^{13}C-NMR, and IR as follows. ^{1}H-NMR (CDCl$_3$) δ (ppm): 5.4 (m, 1H,C$_4$-H), 4.27–4.45 (m, 3H, C$_5$, C$_6$-H), 0.90–2.40 (m, 124H) ^{13}C-NMR δ (ppm): 175.65, 174.56, 171.45, 170.18, 164.92 (C$_1$), 150.01 (C$_3$),
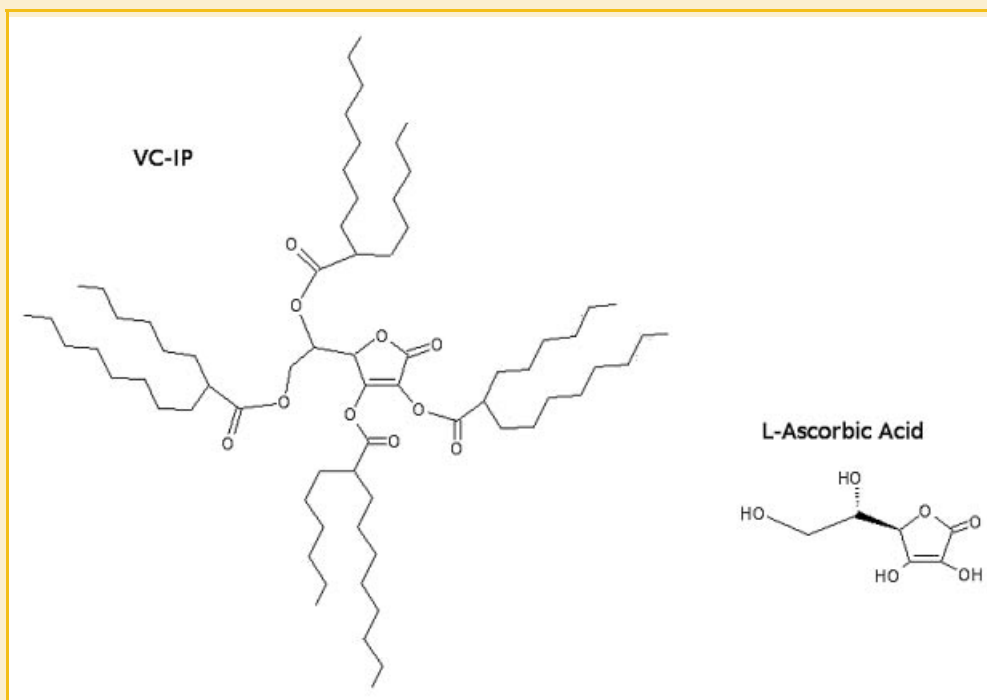
Scheme 1. Molecular formula of VC–IP, MW: 1129.76, as compared with that of L–ascorbic acid.

122.38 (C$_2$), 75.10 (C$_4$), 66.05 (C$_5$), 61.67(C$_6$) IRν (cm^{-1}): 724, 1,101, 1,136, 1,341, 1,379, 1,464, 1,708, 1,746, 1,781, 1,800, 2,862, and 2,960.

THE CHARACTERISTIC OF PHYSICAL CHEMISTRY OF VC–IP

VC-IP is colorless clear liquid, almost soluble in oily materials and thermally stable without deterioration in color. Other characters of VC-IP are as follows: little viscous, density 0.93, viscosity 280 cPs (20°C) and surface tension 26.7 dyne/cm.

SOLUBILITY OF VC–IP

The solubility VC-IP is shown in Table I, VC-IP (5, 10, and 50 wt%) is soluble in various cosmetic oils at temperatures of 25, 50, and 70°C (Table I).

STABILITY OF VC–IP

VC-IP was kept in the thermostat layout at 40 or 60°C for 1 month. It was unchanged on appearance and chrom-phase by sight. The weight was kept at the same value when VC-IP was exposed at 200°C that was measured by Seiko Thermo Gravimetric-Differential Thermal Analysis equipment SSC5200 (Seiko Instruments, Inc., Tokyo) with a speed of increasing temperature 5°C/min, 30–500°C. These findings suggest that VC-IP has excellent thermal stability (Fig. 1).

CELL CULTURE

Human skin keratinocytes HaCaT were kindly provided from Prof. Norbert E. Fusenig of Deutsches Krebsforschungszentrum (Heidelberg, Germany) [Boukamp et al., 1988], and routinely cultured at 37°C in a humidified atmosphere (5% CO$_2$ in air) in Dulbecco's modified Eagle minimum essential medium (DMEM) (Nissui Seiyaku, Tokyo) containing 1 mM L-Arg, supplemented with
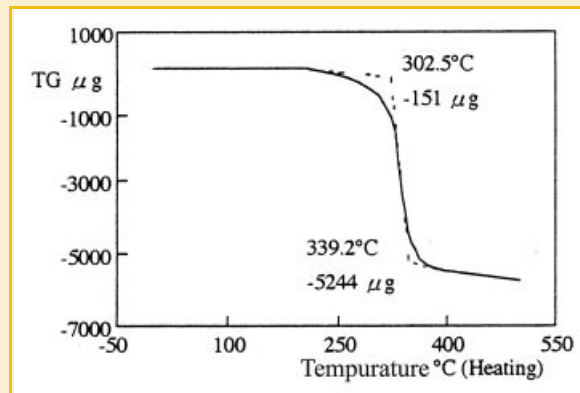

Fig. 1. Stability of VC–IP/VC–IP liquiform was heated at temperatures from 30 to 500°C with a speed of increasing temperature 5°C/min. TG, thermo gravimetric analysis.

10% fetal bovine serum (FBS, GIBCO/BRL Life Technologies), 4 mM L-glutamine (Sigma), 100 U/ml penicillin (Sigma), and 100 µg/ml streptomycin (Nissui Seiyaku). Human melanoma cells HMV-II were kindly gifted by Dr. Kasuga of Tokyo Med. Dent. Univ. [Nakamura et al., 1988] and maintained in Ham F12 medium (Nissui Seiyaku) containing 15% FBS, 2 mM L-glutamine (Sigma), and two above-mentioned antibiotics of the same concentrations. Human skin fibroblasts NHDF were purchased from DaiNippon Pharm., Inc. (Osaka) and were maintained in DMEM supplemented with 10% FBS and similarly two antibiotics. Other cell culture reagents were provided from Sigma Chemical Co. (St. Louis, MO). For each study, cells were plated onto 10-cm tissue culture dishes and grew for 4–7 days up to near 80% confluence. The spent culture medium was replaced by fresh medium at 48 h before the experiment.

UV–IRRADIATION

After the medium was removed, cells were washed three times with phenol red (PR)-free DMEM supplemented with 10% FBS. The cells were irradiated in 200–500 µl of PR-free DMEM with fluorescent lamps in a high-pressure Tecimex apparatus (Yamashita Denso, Inc., Hypersure 200). The emission maximum of the lamp was centered at 200 nm with sheltering of UVB ray by a silica glass filter. The UVA doses effectively received to the vessel bottom by the cell monolayer were evaluated with a radiometer (Verre & Quartz). The control samples were kept in the dark under the same conditions. For WST-1 assay and other analysis, fresh medium containing 10% FBS was added after UV exposure, and the cells were further incubated at 37°C. At predetermined time points, the cells were harvested and analyzed.

CELL VIABILITY ASSAY

Cell viability was evaluated by photometric assay using the formazan-forming redox indicator dye WST-1 (2-(4-iodophenyl)-3-(4-nitrophenyl)-5-(2-disulfophenyl)-2H-tetrazolium, monosodium salt; Dojn Laboratories Co., Kumamoto, Japan). At different time points, cells were rinsed with PR-free DMEM, then incubated for 3 h

TABLE I. Solubility of VC-IP

| | Concentration (wt.%) | | | | | | | | |
| | 5 | | | 10 | | | 50 | | |
	25	50	70	25	50	70	25	50	70
Water		I	I	I	I	I	I		
Glycerol		I	I	I	I	I	I		
Propylene glycol	I	I	I	I	I	I			
1,3-Butylene glycol	I	I	I	1	I	I			
Ethanol	S	S	S	S	S	S	I	S	S
Propylene glycol monocaprylate	S	S	S	S	S	S	S	S	S
Caster oil	S	S	S	S	S	S	S	S	S
Oleic acid	S	S	S	S	S	S	S	S	S
Glycery tri-2-ethylthexanoate	S	S	S	S	S	S	S	S	S
Glycery tri-decanoate	S	S	S	S	S	S	S	S	S
Oleyl alcohol	S	S	S	S	S	S	S	S	S
Decaglyceryl decaoleate	S	S	S	S	S	S	S	S	S
Isopropyl myristate	S	S	S	S	S	S	S	S	S
Com salada oil	S	S	S	S	S	S	S	S	S
Olive oil	S	S	S	S	S	S	S	S	S
Cetyl isooctanoate	S	S	S	S	S	S	S	S	S
Isocetyl myristate	S	S	S	S	S	S	S	S	S
Jojoba oil	S	S	S	S	S	S	S	S	S
Mineral oil (#70)	S	S	S	S	S	S	S	S	S
Squalane	S	S	S	S	S	S	S	S	S

S, soluble; I, insoluble.
Values 25, 50, and 70 are represent temperature (°C).

in PR-free DMEM medium containing 10% WST-1 at 37°C. Cell viability was determined based on mitochondrial conversion of WST-1 to yellowish formazan, being indicative of the number of viable cells [Ishiyama et al., 1996]. The absorbance at 450 nm was read with an absorbance multiplate reader (Bio-Rad^{Q4}, San Jose, CA, Microplate Photometer).

MEASUREMENT OF INTRACELLULAR ROS LEVEL

In order to investigate the influence of VC-IP on the ROS level in HaCaT cells, we used 6-caboxy-2′, 7′-dichlorodihydrofluorescein diacetate (CDCFH) (Molecular Probes, Eugene, OR) as a redox indicator and used fluorometry as a detection system. The CDCFH-DA dye was taken up by cells, esterolyzed to be membrane-impermeable CDCFH, and oxidized to be highly fluorescent CDCF by reaction with ROS such as hydroperoxide and hydrogen peroxide [Szejda et al. 1984].

The cultures were rinsed with PBS(−) and incubated in phenol red-free DMEM containing 7 μM CDCFH-DA for 30 min. The fluorescence intensity of the oxidative form of CDCFH was measured at 534 nm of an emission wavelength after excitation at 510 nm with a fluorescence plate reader CytoFluor 2350 (Millipore, Bedford, MA). The methanol-killed cells were treated as the blank ones. The images of cellular ROS were observed using a fluorescence microscope (Nikon ECLIPSE E 600, Nikon Co.)

8-OXODEOXYGUANOSINE (8-OHdG) ASSAY

Oxidative DNA damage analysis was performed by 8-OHdG assay. Cellular 8-OHdG was measured using a reformative immunofluorescence method based on the previous report [Kimoto et al. 2000]. Briefly, the slides were fixed with 4% paraformaldehyde in PBS (−) (pH 7.4) at room temperature for 25 min and washed again. They were subsequently treated with permeability buffer for 5 min on ice and washed three times with PBS (−). Non-specific binding was blocked with 1.5% normal goat serum, and incubation with the anti-8-OHdG (deoxyguanosine) monoclonal antibody (Nikken SEIL Co. Ltd.) diluted at a rate of 1:50 in goat serum was performed overnight at 4°C. The slides were then incubated with a FITC-conjugated rabbit anti-mouse secondary antibody for 1 h, and observed using a fluorescence microscopy (NIKON ECLIPSE E600).

FLOW CYTOMETRIC ANALYSIS OF CELL APOPTOSIS AND MITOCHONDRIAL MEMBRANE POTENTIALS

Apoptosis of HaCaT cells was detected using Annexin V-FITC kit (Beckman Coulter, USA). In brief, HaCaT cells (1×10^6) were collected and washed twice with PBS. Cells were resuspended in 1 ml of FITC-annexin V solution which was prepared freshly for each time. After incubation for 10 min in the dark at room temperature, propidium iodide (PI) solution was added to the cell suspension prior to analysis. Then cells were analyzed with a COULTER® EPICS® XL™ flow cytometer: display data as two-color dot plot with FITC-Annexin V (green fluorescence, X axis) versus PI (red fluorescence, Y axis).

To detect the reduction of mitochondrial membrane potential in cells, we used MitoCapture™ mitochondrial apoptosis detection kit (BioVision, Inc.). Unfixed, cultured cells were washed in PBS(−), supplemented with MitoCapture™ in incubation buffer. Then cells were incubated for 15 min at 37°C in 5% CO_2, washed, and resuspended in incubation buffer for immediate flow cytometry using a COULTER® EPICS® XL™ flow cytometer. The percentage of MitoCapture™-positive cells was calculated using the EXPO32™ software (Beckman Coulter).

WESTERN BLOTS FOR P53 PROTEINS

One-quarter- to one-half-confluent cultures were collected, rinsed with PBS, pelleted, lysed in 20 mM Tris buffer (pH 7.3) plus 2% sodium dodecyl sulfate (SDS)- plus a protease inhibitor cocktail (Wako Pure Chemical Industries, Ltd, Osaka), and sonically disrupted. Then 40 μg of protein (assayed with the Bio-Rad protein reagent) from each extract was separated by SDS–polyacrylamide gel electrophoresis with precasted 4–20% gradient polyacrylamide gels (Bio-Rad). Gels were electrotransferred to nitrocellulose membranes, where proteins were detected with antibodies specific for p53, followed by peroxidase-labeled secondary antibody (Santa Cruz) and chemiluminescence reagent (Santa Cruz).

COLLAGEN SYNTHESIS

Human skin fibroblasts NHDF were administered with L-2-[³H]proline (Amersham Biotech) in the presence or absence of VC-IP or ascorbic acid (Asc) of 20–50 μM for 24 h, and underwent cytolysis by NaOH treatment and subsequent neutralization. The cell (1×10^6) extract obtained was thoroughly hydrolyzed with collagenase from Clostridium perfringens (Wako Pure Chemical Industries, Ltd), and separated by TCA/tannin treatment and centrifugation to generate the supernatant and precipitate as the collagen fraction and the non-collagen protein fraction, respectively, both of which were evaluated with an Aloka liquid scintillation counter LC-3600 sci.

ENZYMATIC ACTIVITY OF MMPs

After culturing, the conditioned media were collected and clarified by centrifugation. MMP activity was analyzed by zymography, using a procedure described in reference (Sudel et al. 2003). Briefly, 50 μl of conditioned media were mixed with SDS sample buffer, without β-mercaptoethanol, and heated for 37°C/30 min. Normalized samples (30 μg/lane; Bio-Rad protein assay) underwent the standardized electrophoresis in 10% SDS–PAGE containing 0.1% gelatin (Bio-Rad). Molecular weight markers (6–210 kDa), recombinant human latent MMP-9 (92 kDa), and active MMP-9 (83 kDa; Calbiochem) were loaded as positive controls. The gel was washed in 2.5% Triton X-100 (TX)-PBS to remove SDS and renature the proteins, incubated at 37°C for 48 h in an activation buffer (50 mM Tris–HCl, 200 mM NaCl, 10 mM $CaCl_2$; pH 7.5), rinsed in double distilled water, and finally stained for 60 min with 0.25% Coomassie brilliant blue R250 in 40% isopropanol. Gelatinolytic activity was identified as transparent bands on a uniform blue background following destaining in 7% acetic acid, indicating the area where gelatin was digested.

MEASUREMENT OF INTRACELLULAR L-ASCORBIC ACID (Asc)

Cell samples were subjected to homogenization and extraction in the presence of 3% metaphosphoric acid and 0.2% ethanol, followed by

HPLC separation on an ODS column and UV/coulometric electrochemical detector (ECD) detection with 0.1 M KH$_2$PO$_4$-H$_3$PO$_4$ buffer (pH 2.35) containing 0.02% ethanol and 0.1 mM EDTA-2Na as the mobile phase.

STATISTICAL ANALYSIS

All data, expressed as mean ± standard deviation, were processed statistically by the software of SPSS 11.5 for Windows. The differences of the data were considered significant when $P < 0.05$.

RESULTS AND DISCUSSION

IN VITRO CYTOTOXICITY

Before performing the series tests of bio-functions of VC-IP, we evaluated the cell viability of the keratinocytes, to which VC-IP was administered for 48 h. As shown in Figure 2, after cultured in medium containing VC-IP of the varying concentrations, it was found that the survival rates of HaCaT cells were not decreased below a concentration of 5,000 ppm (4,500 μM). This finding suggests that VC-IP has no or scarce cytotoxicity to human skin keratinocytes even at higher concentrations. According to our other experimental results for toxicity in vivo, VC-IP showed LD$_{50}$ > 2,000 mg/kg to rats. VC-IP occurred no irritating reaction to human skin and exerted no significant cytotoxicity to reconstructed three-dimensional skin model (data are not shown). Therefore, as a cosmetic material, VC-IP is very safe (Fig. 2).

SCAVENGING EFFECT OF VC-IP ON UVA-ENHANCED INTRACELLULAR OXIDATIVE STRESS IN HUMAN MELANOCYTES

It has been reported that, VC-IP could suppress UVB, hydrogen peroxide and *tert*-butyl hydroperoxide induced intracellular oxida-

Fig. 3. Repressive effects of VC-IP on intracellular oxidative stress in UVA-irradiated HaCaT cells. A: Human keratinocytes HaCaT were seeded in 24-well plate and cultivated for 24 h, and then administered with VC-IP at 88 ppm for 3 h. The cells were rinsed and further incubated in phenol red-free DMEM containing 7 μM CDCFH-DA for 30 min. Then the cells were irradiated with UVA (100 J/cm²). At 5, 10, and 30 min after UVA-irradiation, the cells were assayed using a fluorescence plate reader (em: 458 nm, ex: 530 nm). Each column and bar represent the mean ± SD of five independent experiments. ***$P < 0.001$ as compared with the non-preadministraed cells. B: HaCaT cells were seeded in a four-well chamber glass and treated as described in (A). At 5, 30 min after UVR, cellular ROS was observed using a fluorescence microscope. Scale bar indicated 30 μm. [Color figure can be viewed in the online issue, which is available at www.interscience.wiley.com.]
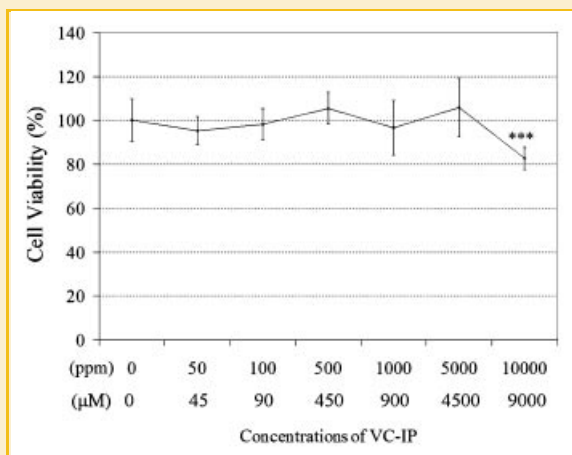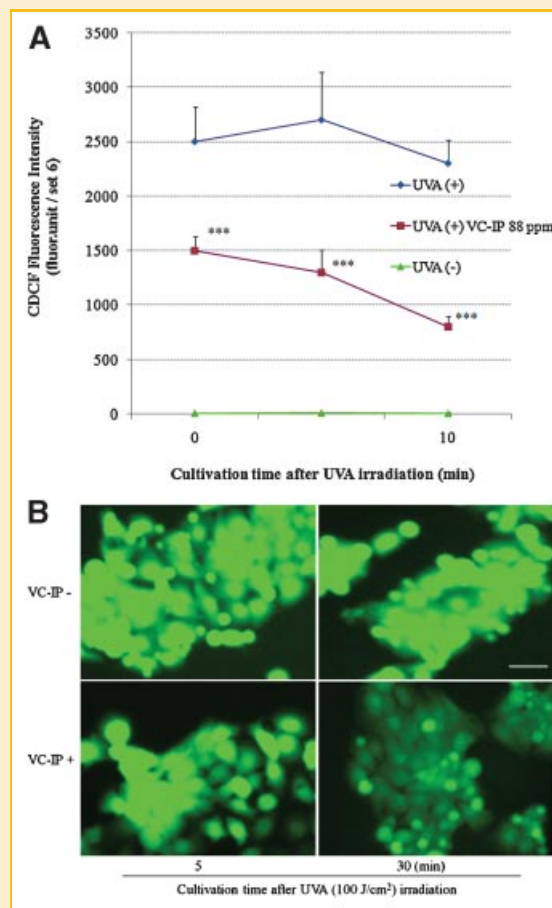

Fig. 2. Effect of VC-IP on cell viability in human skin keratinocytes HaCaT. HaCaT cells were seeded in a 24-well microplate (7,000 cell/well) and were allowed to be grown up to 80% confluence for 24 h. Cells were then incubated with VC-IP at different concentrations for 48 h. The cell viability was estimated by WST-1 assay using a microplate reader. Data are expressed as % of control, and each concentration point and bar represent the mean ± SD of five independent experiments. Control = (0) ***$P < 0.001$ versus the control.

tive stress [Ochiai et al., 2006]. To examine whether VC-IP could influence UVA-induced elevation of intracellular ROS level in human keratinocytes HaCaT, we quantified the intracellular ROS by CDCFH method. As shown in Figure 3A, after irradiation with UVA (100 J/cm²), significant accumulation of intracellular ROS in non-pretreated cells was observed. In the cells pretreated with VC-IP at 88 ppm, the ROS level was markedly reduced to 60%, 48%, and 35% versus the sham-irradiated level at different time points, respectively. Figure 3B shows that at 5 and 30 min after UVA irradiation, the high fluorescence intensity in the non-pretreated HaCaT cells were observed, whereas VC-IP-pretreated cells showed much lower fluorescence intensity. The UVA-induced intracellular ROS enhancement was prevented by addition of 88 ppm VC-IP.
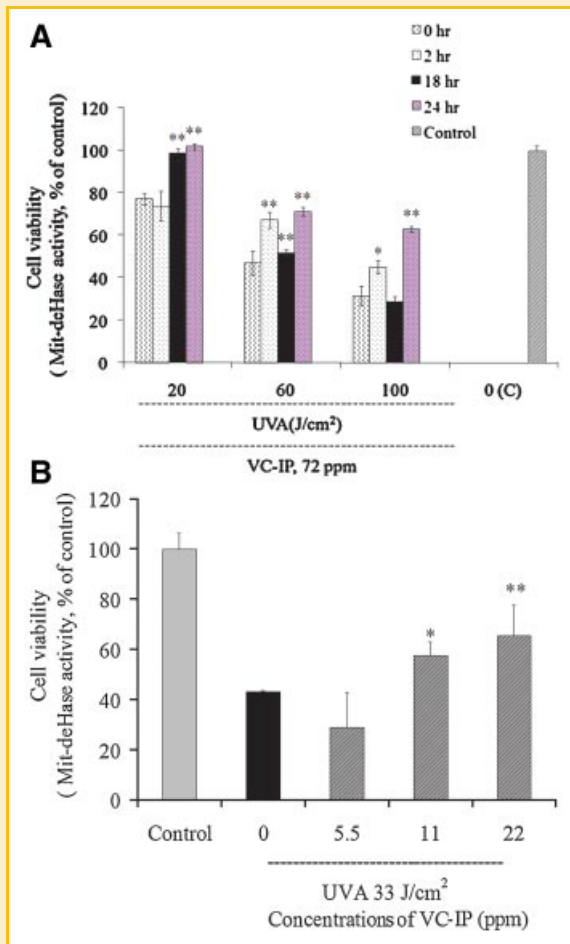
Fig. 4. Repressive effects of VC-IP against UVA-induced cell death in HaCaT cells and HMV-II cells. A: HaCaT cells were seeded and further cultured as in Figure 2. Then cells were previously administered with VC-IP at a final concentration of 72 ppm or none ("0 h" in the figure) for 2, 18, or 24 h. Then cells underwent UVA-irradiation at a dose of 20, 60, or 100 J/cm^2. The control samples were kept in the dark. After 48-h post-irradiational cultivation, cell viability was estimated by WST-1 assay. Data are expressed as % of the control cell-based absorbance, and each column and bar represent the mean $\pm$ SD of three independent experiments ($^{**}P < 0.01$ as compared with 0-h group samples) ($^{*}P < 0.05$, $^{**}P < 0.01$ as compared with "0 (C)"). B: HMV-II human melanoma cells were similarly seeded and further cultured for 24 h. Then the cells were previously administered with VC-IP at different concentrations for 3 h and followed by irradiation with UVA at 33 J/cm^2. The control samples were kept in the dark. Similarly, cell viability was estimated and data are expressed. [Color figure can be viewed in the online issue, which is available at www.interscience.wiley.com.]

CYTOPROTECTIVE EFFECTS OF VC-IP ON UVA-IRRADIATION IN HUMAN KERATINOCYTES HACAT AND HUMAN MELANOCYTES HMV-II

To examine the cytoprotective effect of VC-IP, at 48 h after UVA irradiation, we determined cell viabilities of HaCaT and HMV-II cells which were pre-administered with VC-IP at different time points. As shown in Figure 4A, UVA-irradiation decreased the cell viability in a dose-dependent manner. After irradiated with UVA at the doses of 20, 60, and 100 J/cm^2, the cell viability was reduced to 77%, 47%, and 31% of that of sham-irradiated control, respectively. When the

cells were pre-treated with VC-IP of 72 ppm (65 μM) for 2 h, the cell viability was significantly increased to 71% at 60 J/cm^2 and 47% at 100 J/cm^2 of a UVA irradiance. When the pre-treatment time of VC-IP was further extended to 24 h, the cell viability was markedly increased to 100% at 20 J/cm^2, 69.5% at 60 J/cm^2, and 63.6% at 100 J/cm^2 of UVA irradiance, respectively. When the pre-treatment time of VC-IP was prolonged to 18 h, the cell viability was significantly increased to 99.8% at 20 J/cm^2 and 49.5% at 60 J/cm^2 of UVA. Why the cell viability was lower upon pretreatment with VC-IP at 18 h than those at 2 and 24 h before UVA-irradiation at 60 and 100 J/cm^2? The reason is considered to be that because a doubling time of HaCaT cells is about 20 h, cellular Asc that was esterolytically supplied from VC-IP, at 18 h after administration with VC-IP, is largely expended to achieve continued mitosis, and at this time there may be therefore no enough Asc to scavenge ROS when cells are exposed to strong UVA-irradiation. These results suggested that VC-IP could protect HaCaT keratinocytes from UVA injures, especially upon pretreatment at 24 h before UVA irradiation, suggesting a opportune period necessary for esterolytic conversion of VC-IP into a really active form of the ROS-scavenger such as Asc.

Melanocyte is another very important component cell of skin. Melanocytes protect skin from UV-induced harmful effect through melanogenesis. Here we use human melanoma cells HMV-II which are considered as a good substitute of human normal melanocyte [Nakamura et al., 1988] to observe the cytoprotective effect of VC-IP against UVA injury as shown in Figure 4B. At 48 h after UVA irradiation, HMV-II cell viability was reduced to 43% of that of sham-irradiated control. When the cells were pretreated with VC-IP at concentrations of 2.5, 11, and 22 ppm for 3 h, the cell viability was increased to 29%, 57%, and 65%, respectively. VC-IP significantly enhanced the cell viability at concentrations of 11 and 22 ppm, being marked cytoprotection for human melanocytes.

INHIBITORY EFFECTS OF VC-IP ON PRODUCTION OF 8-OHdG IN THE NUCLEI OF HaCaT CELLS

The formation of 8-OHdG-adducted bases is an oxidative modification of DNA and is considered as a deteriorative consequence of oxidative stress. After UVA irradiation (100 J/cm^2), formation of 8-OHdG markedly became detectable in the nuclei and cytoplasma of HaCaT cells at post-irradiational 1 h, as shown in Figure 5B, most of formed 8-OHdG were accumulated in the nucleus of UVA-irradiated and non-preadministered cell, and then became fadeout or bleached as shown by immunofluorescence stain using anti-8-OHdG antibody. When VC-IP was administered to HaCaT cells at 72 ppm at 24 h before UVA irradiation, the formation of 8-OHdG was significant reduced (Fig. 5A). The result suggested that VC-IP could protect keratinocytes from UVA-caused DNA oxidative damage assumedly through scavenging of UVA-derived ROS by VC-IP or its esterolytic active form.

INHIBITORY EFFECTS OF VC-IP ON UVA-INDUCED APOPTOSIS OF HaCaT CELLS

At 12 h after UVA (100 J/cm^2) irradiation, apoptotic HaCaT cells were identified by double supravital staining with recombinant FITC-conjugated annexin-V and propidium iodide and analyzed by
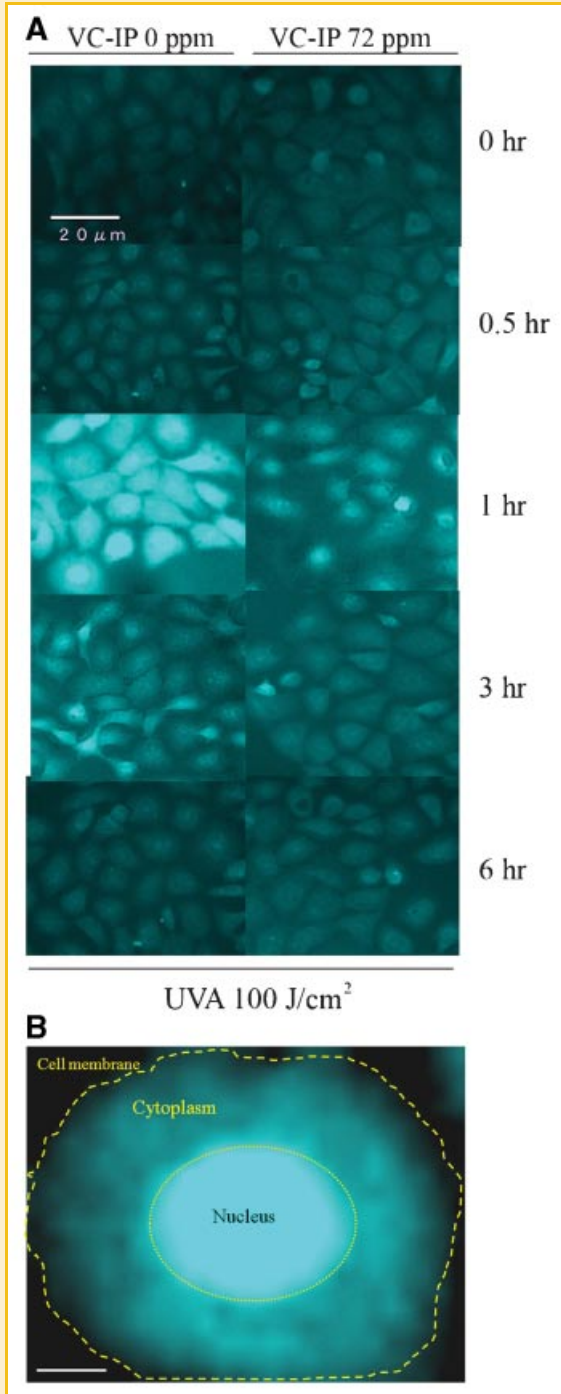
Fig. 5. Inhibitory effects of VC–IP on production of 8–OHdG in HaCaT cells. A: HaCaT cells were seeded on a chamber slide at a density of 8,000 cells/well and cultivated for 24 h. The cells were then irradiated with UVA at 100 J/cm^2 in 200 μl of PR–free DMEM. Cells were further incubated for 0–6 h and then immunostained with anti 8–OHdG monoclonal antibody and visualized with FITC–conjugated anti–IgG antibody. Specimens were observed with a fluorescence microscope. The images are representatives of three independent experiments which showed an 8–OHdG time–lapse pattern similar to one another. B: Magnified image of a single non–pretreated cell at 1 h after UVA–irradiation. Scale bar = 3 μm. [Color figure can be viewed in the online issue, which is available at www.interscience.wiley.com.]

flow cytometry. A middle panel of Figure 6A shows that after UVA irradiation, about 18.9% of cells showed annexin V-positive staining which means those cells underwent early apoptotic change and 45.7% of cells showed annexin V-PI-positive staining, which indicates those cells were suffering from late stage apoptosis and necrosis. In contrast, VC-IP (88 ppm, 24 h)-preadministered cells showed early stage apoptosis for 10.8% out of the total cell population and late stage apoptosis/necrosis for 1.7% (Fig. 6A, the right panel), both being markedly diminished as compared with UVA-irradiated and non-preadministered cells. These results suggested that VC-IP could largely reduce UVA-caused apoptotic and necrotic cell death in keratinocytes.

Mitochondrial alterations, including oxy-radical production and membrane permeability changes, play a pivotal role in UVA-caused cell death and the concomitant oxidative insults [Suschek et al., 2001]. We therefore determined whether VC-IP may modify mitochondrial changes involved in the death of HaCaT cells subjected to UVA irradiation. The green fluorescent dye MitoCapture™ mitochondrial apoptosis detection kit was used to assess mitochondrial membrane potential and then analyzed by flow cytometry. Exposure of cell cultures to UVA irradiation resulted in a significant increase in the amount of FITC-fluorescence in HaCaT cells within 12 h (Fig. 6B, a middle panel). Pre-treatment with VC-IP of 88 ppm at 24 h before UVA irradiation that significantly attenuated the number of apoptotic HaCaT cells (Fig. 6B, a right panel). These findings suggest that the cytoprotective effect of VC-IP is associated with preservation of mitochondrial membrane potential. VC-IP can stabilize mitochondrial function and thereby protect the cells against apoptotic death induced by UVA insults.

EFFECTS OF VC-IP ON UVA-MODULATED APOPTOSIS-RELATED PROTEIN p53 EXPRESSION

The wild-type p53 protein acts as the molecular policeman of the genome by halting the cell cycle to allow repair, or if repair is not possible, promoting cell death by apoptosis. DNA-damaging agents such as UV and ionizing radiation induce high levels of wild-type p53 [Saied and Shamsuddin, 1998]. To determine whether VC-IP prevents UVA-induced above-mentioned response in HaCaT cells, we investigated the levels of wild-type p53 in 40 μg of total protein from each cell extract at 3 h after UVA-irradiation at 100 J/cm^2 by Western blot. The protein bands were scanned and analyzed by an ACT-II software. Figure 7 shows that UVA-modulated expression of p53 proteins was significantly suppressed in HaCaT cell 24 h pretreated by VC-IP in a concentration-dependent manner. The expression of p53 proteins in VC-IP (44 and 88 ppm)-pretreated cells was as low as 49% and 12% of the control, respectively. This result suggests that VC-IP can stabilize UVA-activated wild-type p53 proteins to prevent apoptosis.

PROMOTIVE EFFECTS OF VC-IP ON COLLAGEN SYNTHESIS IN HUMAN SKIN FIBROBLASTS NHDF

The loss of collagen is considered as the characteristic histological finding in aged skin. To investigate whether VC-IP could influence type-IV collagen synthesis in human skin fibroblasts NHDF, we quantified the collagen level of NHDF after VC-IP or Asc treatment. Figure 8 shows that after NHDF cells were treated with VC-IP at the
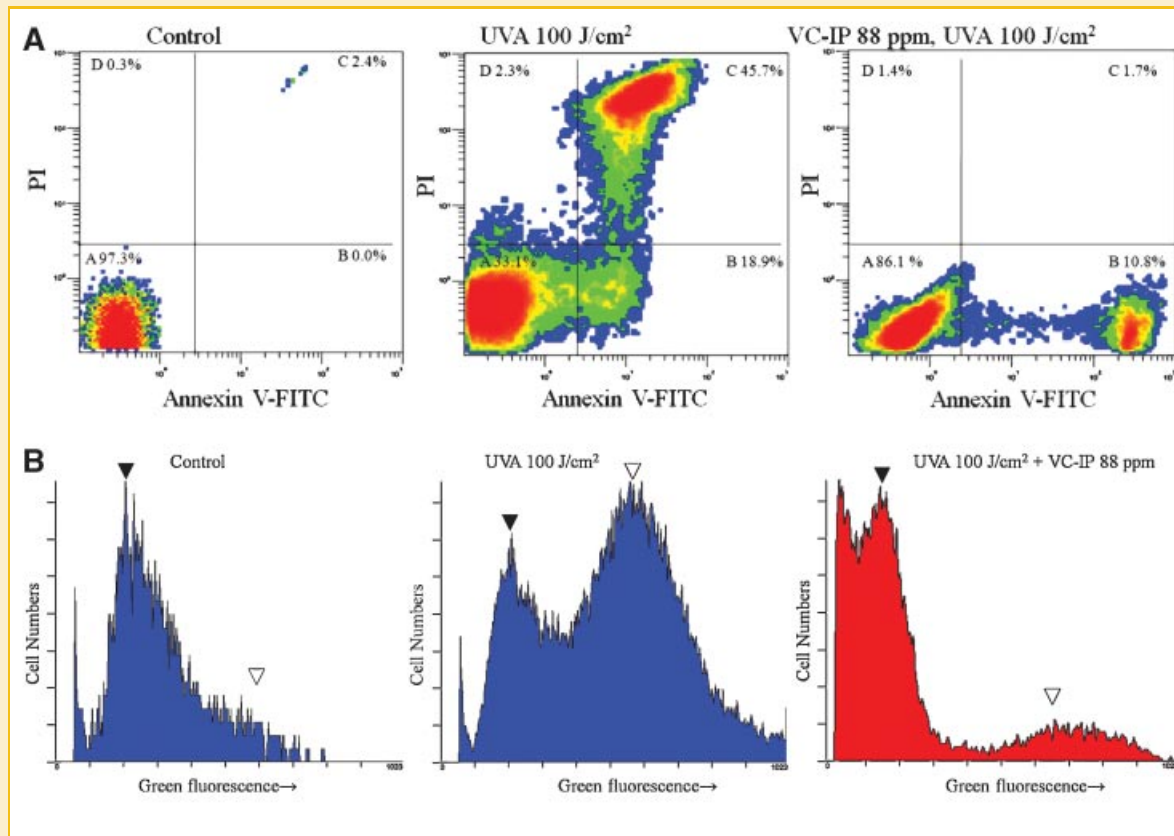
Fig. 6.   Repressive effects of VC–IP on UVA–induced apoptosis–associated molecular symptoms in HaCaT keratinocytes and HMV–II cells. A: HaCaT cells were seeded in six–well plates at a density of 50,000 cells/well and cultivated for 18 h. At 24 h after incubation with VC–IP at 88 ppm, the cells were irradiated by UVA. Cells were further incubated for 12 h and then double–stained with Annexin V–propidium iodide (PI). Then 10,000 cells were immediately analyzed by flow cytometry for membrane permeability–promoted disruption and membrane–constituting phosphatidylserine inner–to–outer translocation. The dot–images are representatives of three independent experiments with similar tendencies. Area A, Normal cells; Area B, Apoptotic cells (early stage); Area C, Apoptotic cells (late stage) and necrotic cells. B: HaCaT cells were treated in the same manner as described in Figure 6A. After UVA irradiation, cells were stained with the green fluorescent dye MitoCapture™. The mitochondrial membrane potential was immediately analyzed by flow cytometry. The histograms are representatives of three independent experiments with similar tendencies. (▼) Normal cells; (▽) apoptotic cells. [Color figure can be viewed in the online issue, which is available at www.interscience.wiley.com.]

concentrations of 10, 20, and 50 μM for 24 h, the collagen synthesis in 1×10^6 cells was markedly increased to 144.6%, 174.1%, and 193.3% of the control, respectively. The collagen synthesis levels of Asc (20 and 50 μM)–administrated cells (1×10^6 cells) were enhanced to 110% and 127%, respectively. These results indicate that VC–IP could largely promote collagen synthesis in human skin fibroblasts NHDF in a concentration–dependent manner. VC–IP showed a collagen–increasing activity more potent than Asc at the same concentrations.

INHIBITORY EFFECTS OF VC–IP ON MMPs IN HUMAN SKIN FIBROBLASTS NHDF

The expression and functional activities of MMP-2 and MMP-9 were known to drive specifically collagen type-IV cleavage [Sancéau et al., 2003; Marin-Castaño et al., 2005]. To examine whether VC–IP could influence MMPs activity in human skin fibroblasts, we quantified the activity of MMP-2 and MMP-9 of NHDF cells after incubation with VC–IP or Asc. As shown in Figure 9, the activities of MMP-2 and MMP-9 were obviously decreased by VC–IP at 10, 20, and 50 μM and Asc at 20 and 50 μM. Both MMP-2

and MMP-9 levels of VC–IP-treated cells are significantly lower than Asc at the same concentrations. The result indicates that VC–IP not only promotes the collagen synthesis but also reduce the activity of MMPs to prevent collagen degradation.

CONVERSION ABILITY OF VC–IP TO INTRACELLULAR AsA IN NHDF FIBROBLASTS

To examine whether VC–IP permeates through the plasma membrane to be transformed to Asc in NHDF fibroblasts, we observed the concentrations of intracellular Asc in VC–IP- or Asc-treated NHDF cells by HPLC separation and UV/coulometric ECD detection. Figure 10 shows that the intracellular Asc concentrations of VC–IP (5, 10, 20, and 50 μM)–pre-treated cells were 2.18, 5.48, 10.15, and 9.46 nmol/10^6 cells, respectively. The intracellular Asc levels of NHDF cells which treated with Asc at higher concentrations of 20, 50, and 100 μM, were 0.86, 1.42, and 1.29 nmol/10^6 cells, respectively. VC–IP enhanced intracellular Asc through its persistent conversion to Asc, than administration with Asc. This finding indicates a possibility that VC–IP could cross the hydrophobic plasma membrane and is transformed to the major antioxidant Asc in cells.
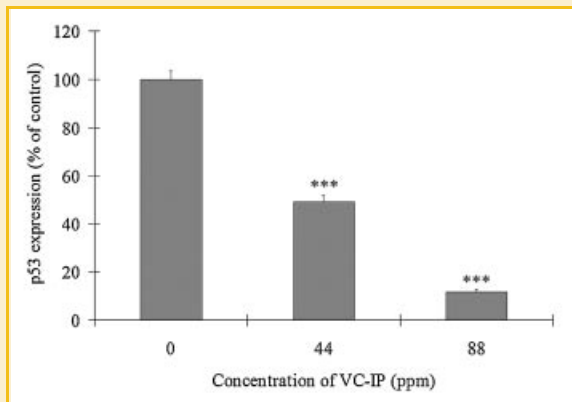
Fig. 7. Inhibitory effects of VC-IP on UVA-induced expression of p53 protein as shown by Western blot analysis. HaCaT cells were treated in the same manner as described in Figure 6A. At 3 h after UVA irradiation, about 1×10^7 cells were collected and subjected to Western blotting. Then the transferred membrane was scanned for the density and analyzed with an ACT-II software. Data are expressed as % of the basal density, and each column and bar represent the mean $\pm$ SD of three independent experiments. ***$P < 0.01$ as compared with the control (0).
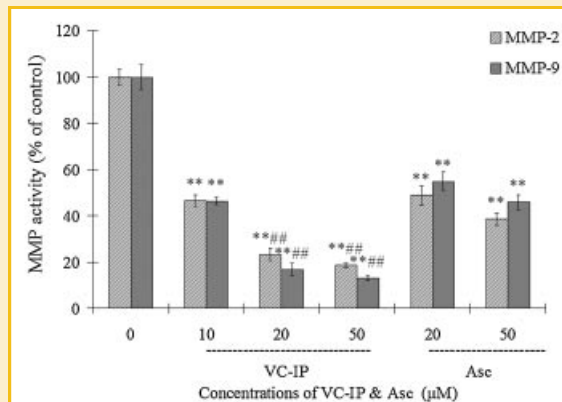

Fig. 9. Inhibitory effect of VC-IP on MMPs activity in human skin fibroblasts NHDF. NHDF cells were cultured in serum-free conditioned media for 48 h in the presence or absence of VC-IP and Asc at different concentrations, and subjected to zymography under non-reduced conditions containing 0.2% gelatin, followed by staining and subsequent densitometry. Activity of MMP-2 and MMP-9 are expressed as % of the control, and each column and bar represent the mean $\pm$ SD of three independent experiments. **$P < 0.01$ as compared with the control group; ##$P < 0.01$ as compared with Asc samples at the same concentration.

In conclusion, the new lipophilic Asc derivative, 2,3,5,6-O-tetra-2′- hexyldecanoyl-L-ascorbic acid (VC-IP) that is a colorless and transparent liquid has the extremely high thermal stability in cosmetic formulations without losing the favorable Asc-based activities. VC-IP did not reduce the survival rates of HaCaT cells even at a concentration as high as 5,000 ppm (4,500 μM). VC-IP significantly protected human skin cells such as HaCaT keratinocytes and HMV-II pigment cells against UVA-induced cell death in
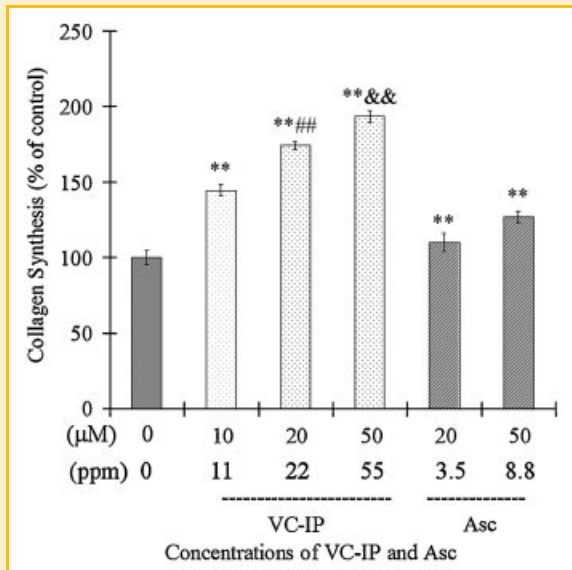

Fig. 8. Promotive effect of VC-IP on collagen synthesis in human skin fibroblasts NHDF. NHDF cells were seeded in a 24-well microplate (20,000 cell/well) and were allowed to be grown up to 80% confluence for 24 h. Cells were then incubated with VC-IP or Asc at different concentrations for 24 h. Collagen synthesis in NHDF cells (1×10^6) was performed by radio-labeled proline incorporation method. Data are expressed as % of the control radio-activity, and each column and bar represent the mean $\pm$ SD of three independent experiments. **$P < 0.01$ as compared with the control; ##$P < 0.01$ as compared with Asc 20 μM samples; &&$P < 0.01$ as compared with Asc 50 μM samples.
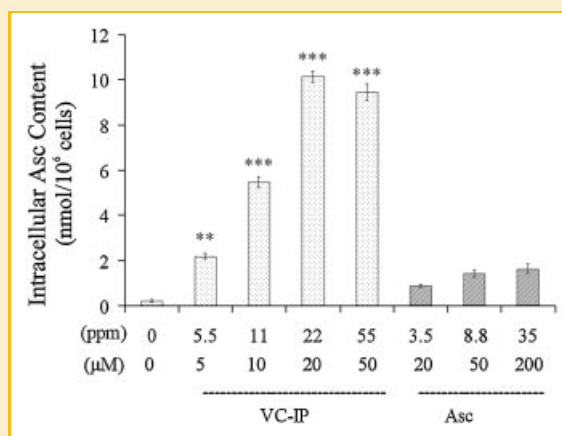

Fig. 10. Conversion ratio of VC-IP to intracellular Asc in NHDF fibroblasts. NHDF cells were administered with VC-IP or Asc at different concentrations for 2 h, and were subjected to homogenization and extraction, followed by HPLC separation and UV/coulometric ECD detection. Data are expressed as % of the control value, and each column and bar represent the mean $\pm$ SD of three independent experiments (**$P < 0.01$ as compared with Asc 20 μM samples; &&$P < 0.01$ as compared with Asc 50 μM samples).

vitro as shown by WST-1 method. The mitochondrion and the plasma membrane, which are considered to be two main sites of ROS production [Agarwal et al., 2005], may be dually protected by lipophilic Asc derivatives. It has been reported that there was a relationship between structure and bio-activities of Asc. Lipophilicity is an important determinant of antioxidant activity as it can regulate membrane permeability and component distribution in lipid bilayer membrane. According to our previous study, VC-IP could decrease UVB-induced photo-oxidation on human sebum such as squalene (data are not shown). In the present study, VC-IP was demonstrated to enhance intracellular accumulation of Asc, assumedly through esterolytic conversion to Asc, more markedly than administration with Asc itself being susceptible to oxidative degradation. Flow cytometric analysis showed that VC-IP could stabilize the plasma membranes and mitochondria membrane potential to prevent UVA-induced apoptosis. These effects may ensue from the abilities of VC-IP to repress production of 8-OHdG and down-regulate the expression of apoptosis-related gene p53. VC-IP also showed a promotive effect on collagen synthesis and a repressive effect on MMP activities.

Thus application with VC-IP may alleviate skin damage following physiologic doses of UVA irradiation, and should be adopted in the preventative and protective strategies against UVA injuries.

REFERENCES

Agarwal A, Prabakaran SA, Said TM. 2005. Prevention of oxidative stress injury to sperm. J Androl 26:654–660.

Besaratinia A, Kim SI, Bates SE, Pfeifer GP. 2007. Riboflavin activated by ultraviolet A1 irradiation induces oxidative DNA damage-mediated mutations inhibited by vitamin C. Proc Natl Acad Sci USA 104:5953–5958.

Boukamp P, Petrussevska RT, Breitkreutz D, Hornung J, Markham A, Fusenig NE. 1988. Normal keratinization in a spontaneously immortalized aneuploid human keratinocyte cell line. J Cell Biol 106:761–771.

Fisher GJ, Kang S, Varani J, Bata-Csorgo Z, Wan Y, Datta S, Voorhees JJ. 2002. Mechanisms of photoaging and chronological skin aging. Arch Dermatol 138:1462–1470.

Honda A, Abe R, Makino T, Norisugi O, Fujita Y, Watanabe H, Nishihira J, Iwakura Y, Yamagishi S, Shimizu H, Shimizu T. 2008. nterleukin-1beta and macrophage migration inhibitory factor (MIF) in dermal fibroblasts mediate UVA-induced matrix metalloproteinase-1 expression. J Dermatol Sci 49:63–72.

Ichihashi M, Ueda M, Budiyanto A, Bito T, Oka M, Fukunaga M, Tsuru K, Horikawa T. 2003. UV-induced skin damage. Toxicology 189:21–39.

Ishiyama M, Tominaga H, Shiga M, Sasamoto K, Ohkura Y, Ueno K. 1996. A combined assay of cell viability and in vitro cytotoxicity with a highly water-soluble tetrazolium salt, neutral red and crystal violet. Biol Pharm Bull 19:1518–1520.

Kim JH, Cho YH, Park SM, Lee KE, Lee JJ, Lee BC, Pyo HB, Song KS, Park HD, Yun YP. 2004. Antioxidants and inhibitor of matrix metalloproteinase-1 expression from leaves of Zostera marina L. Arch Pharm Res 27:177–183.

Kimoto T, Koya S, Hino K, Yamamoto Y, Nomura Y, Micallef MJ, Hanaya T, Arai S, Ikeda M, Kurimoto M. 2000. Renal carcinogenesis induced by ferric nitrilotriacetate in mice, and protection from it by Brazilian propolis and artepillin C. Pathol Int 50:679–689.

Kurata S, Senoo H, Hata R. 1993. Transcriptional activation of type I collagen genes by ascorbic acid 2-phosphate in human skin fibroblasts and its failure in cells from a patient with alpha 2(I)-chain-defective Ehlers-Danlos syndrome. Exp Cell Res 206:63–71.

Liardet S, Scaletta C, Panizzon R, Hohlfeld P, Laurent-Applegate L. 2001. Protection against pyrimidine dimers, p53, and 8-hydroxy-2'-deoxyguanosine expression in ultraviolet-irradiated human skin by sunscreens: Difference between UVB + UVA and UVB alone sunscreens. J Invest Dermatol 117:1437–1441.

Marin-Castaño ME, Csaky KG, Cousins SW. 2005. Nonlethal oxidant injury to human retinal pigment epithelium cells causes cell membrane blebbing but decreased MMP-2 activity. Invest Ophthalmol Vis Sci 46:3331–3340.

Molho-Pessach V, Lotem M. 2007. Ultraviolet radiation and cutaneous carcinogenesis. Curr Probl Dermatol 35:14–27.

Nakamura T, Seki S, Matsubara O, Ito S, Kasuga T. 1988. Specific incorporation of 4-S-cysteinylphenol into human melanoma cells. J Invest Dermatol 90:725–728.

Negishi T, Kawai K, Arakawa R, Higashi S, Nakamura T, Watanabe M, Kasai H, Fujikawa K. 2007. Increased levels of 8-hydroxy-2'-deoxyguanosine in Drosophila larval DNA after irradiation with 364-nm laser light but not with X-rays. Photochem Photobiol 83:658–663.

Ochiai Y, Kaburagi S, Obayashi K, Ujiie N, Hashimoto S, Okano Y, Masaki H, Ichihashi M, Sakurai H. 2006. A new lipophilic pro-vitamin C, tetra-isopalmitoyl ascorbic acid (VC-IP), prevents UV-induced skin pigmentation through its anti-oxidative properties. J Dermatol Sci 44:37–44.

Saied IT, Shamsuddin AM. 1998. Up-regulation of the tumor suppressor gene p53 and WAF1 gene expression by IP6 in HT-29 human colon carcinoma cell line. Anticancer Res 18:1479–1484.

Sancéau J, Truchet S, Bauvois B. 2003. Matrix metalloproteinase-9 silencing by RNA interference triggers the migratory-adhesive switch in Ewing's sarcoma cells. J Biol Chem 278:36537–36546.

Sudel KM, Venzke K, Knussmann-Hartig E, Moll I, Stab F, Wenck H, Wittern KP, Gercken G, Gallinat S. 2003. Tight control of matrix metalloproteinase-1 activity in human skin. Photochem Photobiol 78:355–360.

Suschek CV, Briviba K, Bruch-Gerharz D, Sies H, Kröncke KD, Kolb-Bachofen V. 2001. Even after UVA-exposure will nitric oxide protect cells from reactive oxygen intermediate-mediated apoptosis and necrosis. Cell Death Differ 8:515–527.

Szejda P, Parce JW, Seeds MS, Bass DA. 1984. Flow cytometric quantitation of oxidative product formation by polymorphonuclear leukocytes during phagocytosis. J Immunol 133:3303–3307.

Tai A, Kawasaki D, Goto S, Gohda E, Yamamoto I. 2003. Vitamin C activity in guinea pigs of 6-O-acyl-2-O-alpha-D-glucopyranosyl-L-ascorbic acids with a branched-acyl chain. Biosci Biotechnol Biochem 67:1675–1682.

Thomas FH, Leask R, Srsen V, Riley SC, Spears N, Telfer EE. 2001. Effect of ascorbic acid on health and morphology of bovine preantral follicles during long-term culture. Reproduction 122:487–495.

Wlaschek M, Briviba K, Stricklin GP, Sies H, Scharffetter-Kochanek K. 1995. Singlet oxygen may mediate the ultraviolet A-induced synthesis of interstitial collagenase. J Invest Dermatol 104:194–198.

Yu H, Xia Q, Yan J, Herreno-Saenz D, Wu YS, Tang IW, Fu PP. 2006. Photoirradiation of polycyclic aromatic hydrocarbons with UVA light−A pathway leading to the generation of reactive oxygen species, lipid peroxidation, and DNA damage. Int J Environ Res Public Health 3:348–354.